 MCB, vol.11, no.2, pp.87-100, 2014

Anisometry Anterior Cruciate Ligament Sport Injury Mechanism Study: A Finite Element Model with Optimization Method

Na Li[*], **Wei Wang**[*], **Bin Ye**[*] **and Song Wu**[†,‡]

Abstract: ACL damage is one the most frequent causes of knee injuries and thus has long been the focus of research in biomechanics and sports medicine. Due to the anisometric geometry and functional complexity of the ACL in the knee joint, it is usually difficult to experimentally study the biomechanics of ACLs. Anatomically ACL geometry was obtained from both MR images and anatomical observations. The optimal material parameters of the ACL were obtained by using an optimization-based material identification method that minimized the differences between experimental results from ACL specimens and FE simulations. The optimal FE model simulated biomechanical responses of the ACL during complex combined injury-causing knee movements, it predicted stress concentrations on the top and middle side of the posterolateral (PL) bundles. This model was further validated by a clinical case of ACL injury diagnosed by MRI and arthroscope, it demonstrated that the locations of rupture in the patient's knee corresponded to those where the stresses and moments were predicted to be concentrated. The result implies that varus rotation played a contributing but secondary role in injury under combined movements, the ACL elevation angle, is positive correlated with the tensional loading tolerance of the ACL.

Keywords: Finite element model, Anterior cruciate ligament, Anisometry, Optimization, Injury mechanism.

1 Introduction

The anterior cruciate ligament (ACL) is an important stabilizing structure of the knee joint that facilitates various body movements while also supporting the entire weight of the body. During knee joint movement, the ACL mainly provides sta-

[*] Radiology Department, Xiangya No.3 Hospital, Central South University, ChangSha, China.
[†] Orthopedics Department, Xiangya No.3 Hospital, Central South University, ChangSha, China.
[‡] Corresponding author. E-mail: Songwu12@vip.163.com

bility and limits forward translation, valgus or varus rotation, hyperextension, and rotation of the tibia. However, in activities such as sports, the knee joint can be subjected to complicated movements that may combine all of these types of motion; when these movements are extreme, the ACL is often damaged or ruptured. Indeed, ACL damage or rupture is one the most frequent causes of knee injuries and thus has long been the focus of research in biomechanics and sports medicine [1,2,3].

Due to the anatomical and functional complexity of the ACL in the knee joint, it is usually difficult to experimentally study the biomechanics of ACLs. Instead, it is often necessary to investigate ACL behavior with computational methods such as finite element (FE) modeling. During the past decade, several three dimensional FE models of the knee joint that also incorporate the ACL have been successfully used to predict body responses to injury-producing conditions [4,5,6,7]. Such predictions are not possible with surrogate or animal experiments. More importantly, these computational models are the only tools with which experimental results from animal or cadaveric studies can be extrapolated to the living human body.

However, FE models of ACLs are limited because they ignore detailed anisometric geometry of the functional fiber bundles in the ACL. In fact, the ACL is composed of fiber bundles with complex anatomy and mechanical behaviors that enable the knee to perform complicate movements. For example, Amiri et al. (2011), Hosseini et al. (2009) and Gabriel et al. (2004) have reported that in multi-axial rotation and uni-axial loading of the knee, the fiber bundles of the ACL exhibit different patterns of stress distribution and elongation [8,9,10]. These findings emphasize functional specificity of specific fiber bundles within the ACL. Therefore, it is essential to incorporate more realistic anatomy and material properties of the fiber bundles in the FE models of ACLs in order to simulate and study the complex and variable functional patterns of the ACL during knee movement.

The anatomy of the ACL fiber bundles can be obtained by high resolution imaging techniques, such as MRI, and anatomical observation. The complex mechanical properties of the ACL fiber bundles, however, are technically challenging to quantify. Recently, Hu et al. (2009) and Guan et al. (2011) quantified complex material parameters of human placental tissue and rat skull, respectively, by using an optimization technique that reduced the average difference between the experimental and simulation data in specimen-specific FE modeling [11,12].

Thus, in this study we aimed to build an anatomically-detailed three dimensional (3D) FE model of the ACL with accurate material parameters and to use this model to quantitatively simulate the biomechanical response of the ACL during injury-causing complex movements of the knee joint. Furthermore, this FE modeling was validated by comparing the simulated ACL injury with that of a patient whose

ACL was partially ruptured during combined knee movements of varus and internal rotations and flexion. This work predicted a stress concentration in the PL bundles with a maximum of thevon-mises stress and maximum moments of the PL and AM bundles. To further investigate how different movements contribute to kinematic knee injury mechanisms, individual varus and uniaxial rotations were simulated by this model. According to these predictions, internal rotation played the most important role in the combined-motion injury, while varus rotation contributed little to ACL injury. Interestingly, the stress due to a combination of varus and internal rotations was higher than the sum of their individual stress components, indicating a synergistic effect of the stresses due to these two movements.

2 Method

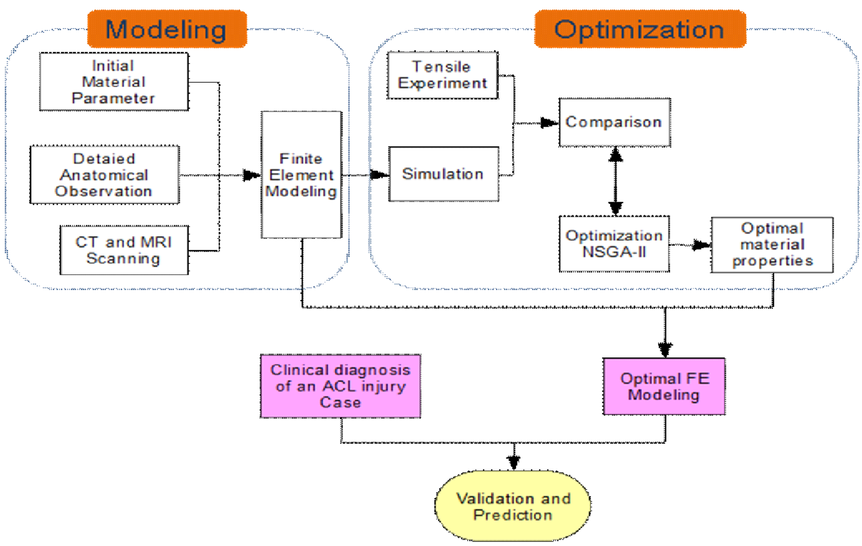

Figure 1: Flowchart of steps to determine mechanical properties of the ACL. Tensile testing, anatomically detailed FE modeling and optimization were performed.

Figure 1 outlines how the anatomical detailed ACL model was developed. The initial geometry was obtained from CT and MRI scans and detailed anatomical observation. An initial material was selected for the FE model and then optimized with an NSGA-II optimization method to reduce the difference between quasi-static and dynamic tensile testing results and FE model simulation results. After optimization, a more representative material parameter was obtained and implemented into the final FE model, which was validated against an actual ACL injury.

2.1 Finite element modeling

The 3-D geometry data of the model developed herein were obtained by MRI scanning (MAGNETOM Avanto 1.5T MRI) for the ACL and CT (Brilliance CT Philips 64 Channels Scanner) for the bones. The CT and MRI images were taken from a patient whose ACL was partially ruptured during combined knee movements of varus and internal rotations and flexion. All images were reconstructed in 3-D by MIMICS (Version 12, Materialise Inc., Leuven, Belgium). To refine the geometry of the model, the 3-D reconstruction of the CT and MRI images were fine-tuned by clinicians from the Orthopedics Department of the No. 3 Xiangya hospital based on anatomical observations on cadavers.

2.2 Optimization

The donor knee joint was from a 34-year-old male and a 38-year-old female cadavers 4 hours after death. To improve the simulation biofidelity of knee joint movement, the femoral lateral condyle and the tibia plateau were cut into a cuboid and embedded in an acrylic denture resin, then clamped to the top and lower grips of MTS . As shown in Figure 2A, the anatomically stretched was shown in Figure 2B, which loading angle is same to the FE model simulation. A load cell below the lower clamp measured the reaction force (accuracy of 0.0001 N). Extension was measured by an MTS displacement transducer; the quasi-static testing with a strain rate of 0.5 mm/min, the dynamic testing with a strain rate of 100mm/min. To obtain more reliable viscoelastic material properties, the reported tensile experiment from Noyes were utilized in optimization [13] (with permission).

The reaction force and global tissue extension of ACL tissue are measured during the tensile experiment. The geometry of the ACL does not have regular symmetry. Instead of the traditional curve-fitting which ignored the actual ACL geometry, in this study, the optimization of FE modeling was developed, material parameters μ and α, which present hyperelastic part from Ogden theory, G and β which present viscoelastic part from the Christensen were set as input variables in the ACL FE model, the force-displacement curves were calculated and set as output in optimization processing, the output was compared with the tensile experimental data.

The objective function utilized a least square method to minimize the average error between the biomechanical experimental results and the node-force curve output from the anatomical detailed FE modeling of ACL, as shown in Eq. (1):

$$E = \sqrt{\sum_{i=1}^{n} (f_{mi} - f_{ei})^2 \Big/ 2} \tag{1}$$

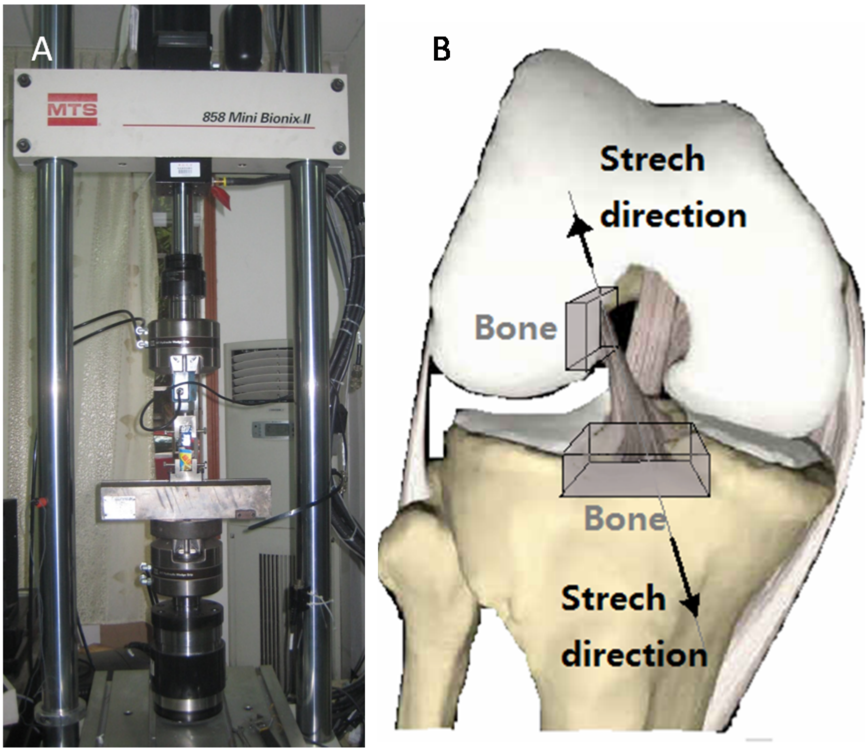

Figure 2: ACL specimen with the media condyle and tibia plateau embedded in acrylic denture resin, the figure 2A shows the MTS machine, the figure 2B shows how to the ACL specimens be fixed on the MTS

where f_{ei} indicates the values measured from tensile experiments, f_{mi} indicates the corresponding force values calculated from the FE model, and n indicates the number of measured data points. An optimization software (ModeFRONTIER, Esteso, Srl, Italy) was utilized to automatically modify the input variables μ and α, β and G then the new key file was input into the LS-DYNA solver. A genetic algorithm-based method (NSGA-II) is a fast and elitist multi-objective evolutionary algorithm [14]. NSGA-II implements elitism for multi-objective searches using an elitism-preserving approach. Elitism is introduced to store all non-dominated solutions discovered so far, beginning with the initial population. Elitism enhances convergence properties towards the true Pareto-optimal set. The algorithm implements a modified definition of dominance in order to solve constrained multi-objective problems efficiently. At the end of the optimization, the optimal material parameters obtained from this procedure are used as input into the FE model. This process is desired to judge the validity of validation against an MRI and arthroscopic observation of an injured knee.

3 Result

3.1 Test result

To improve the simulation biofidelity of knee joint movement, the ACL specimens were anatomically stretched (Figure 2B), and an extension (mm)-force (N) curve was produced until ACL failure occurred (Figure 3). The failure point was defined as the time at which the reaction force reached its maximum value, while sub-failure damage of the ACL occurred at two peak points before total failure. The force-extension curve and video data indicated that the functional bundles of the ACL ruptured successively under increased tensile loading.

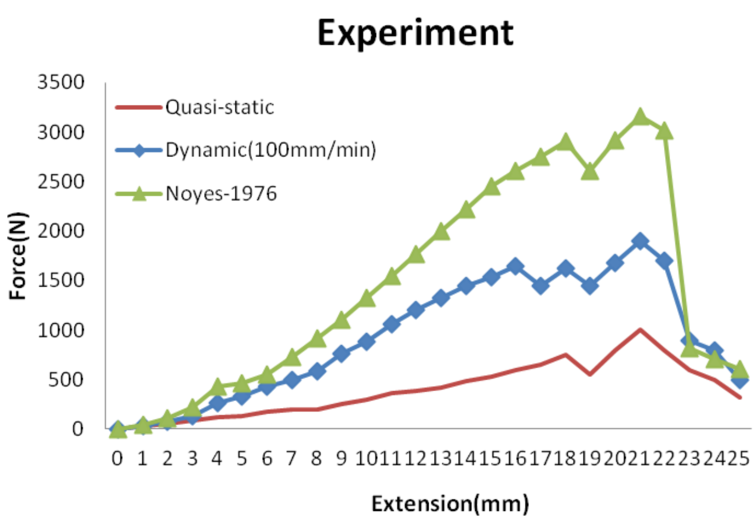

Figure 3: Force-extension curves from experiments, the red curve is quasi-static tensile experiment, the blue color is dynamic experiment in 100mm/min, and the green color curve is from Noyes's report (with permission), the velocity is 200mm/min.

3.2 Material Properties Optimization

Material parameters were calculated from curve fitting before the first peak point. As for quasi-static material properties, according the Ogden theory, the hyperelastic material parameters α and μ were 3.26 and 2.23 MPa. To obtain the viscoelatic material parameters, the dynamic experiment (100mm/min) and literature experiment data were calculated in optimization, β and G were 1.52 and 1.89MPa respectively. Figure 4 shows the comparison between the test results and the optimization results; the errors E were calculated by Eq(1) were 143N in velocity 100mm/min, 84.4N in quasi-static simulation, 193.2N in optimal FE simulation with Noyes's experiment. To obtain accurate material properties, the material parameters were caculated by reversing engineering with the NSGA-II optimization method. The mean square error of force between experimental measurements and simulation results was set as an objective function E and were minimized in the optimization. considering the tensile testing results were only obtained from two fresh cadavers, literature experiment data on ACL were calculated with permission from author (Noyes 1976)[13], the optimization method calculated the material parameter robustly in these three curves with reversing engineering. Therefore, the material parameters deduced for this study are enough believable.

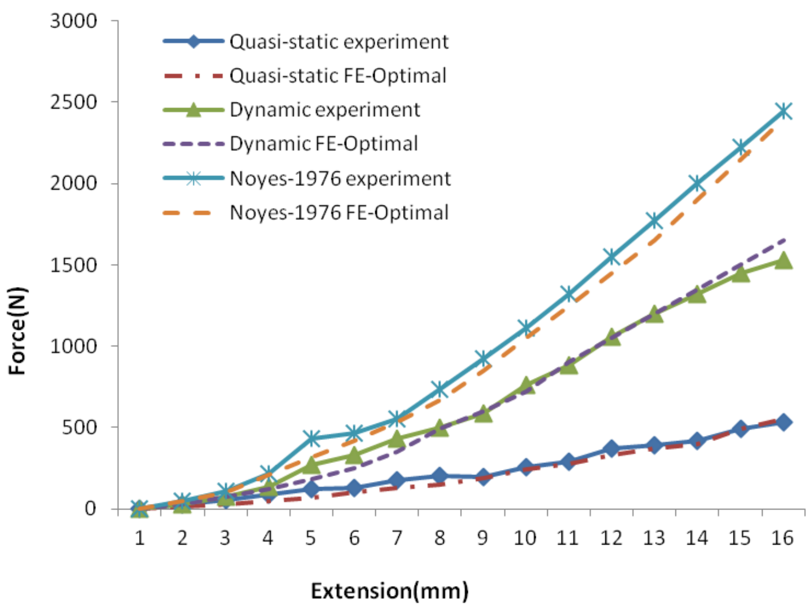

Figure 4: Comparison of stress from the tensile experiments and the FE model with optimization method.

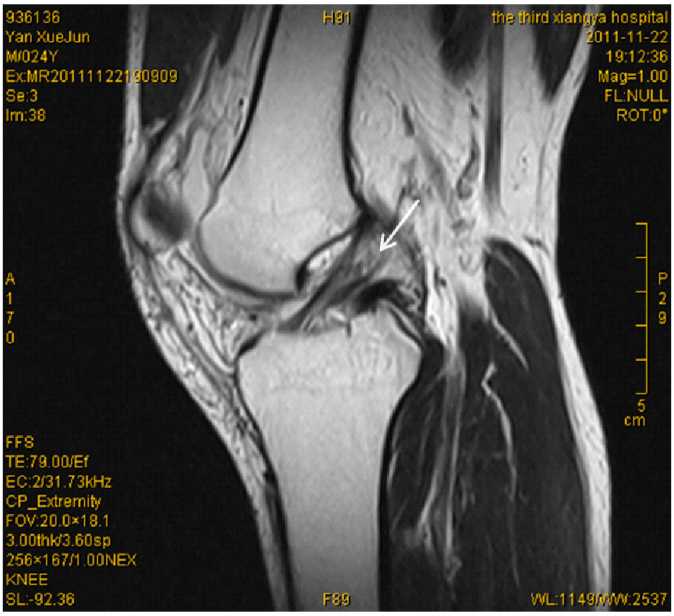

Figure 5: MR image showing the injury region in the top of PL bundle.

3.3 Validation and Injury mechanism

A patient who injury his left knee joint in a badminton sport suffering an internal rotation combined with varus movement, the incomplete ACL rupture injury in the study was detected by MRI and arthroscopy. As illustrated in Figure 5, the ACL fibrous signal was partially interrupted at the top of the PL bundles, which had been directly verified by arthroscopy (Figure 6).

Figure 7A revealed the stress distribution determined from the FE model under combined movements. The model shows a high concentration of stress at the same site as the injury that was revealed by MRI and arthroscopy. Under combined loading, the maximum stress is 589.7 MPa and the maximum moments of the PL and AM bundles are 59.5 Nm and 27.33 Nm (Figure 8B), the maximum force of the PL and AM bundles are 1183N and 862N respectively (Figure 8A). In the simulation of only Internal rotation movement, stress was concentrated on the top and middle of the PL bundles, as show in Figure 7B, the maximum stress is 193.5 MPa, the maximum force of the PL and AM bundles are 450N and 227N, as shown in Figure 8A, the maximum moment of the PL bundle is 11.6 Nm, and the maximum moment of the AM bundle is 3.2 Nm, as shown in Figure 8B. Under varus loading, the simulation also predicts that stress is concentrated on the top and middle of the PL

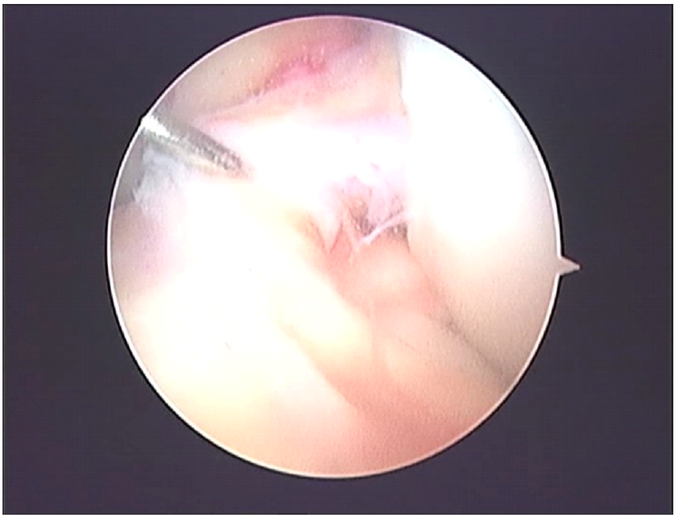

Figure 6: Arthroscopy showing the top of PL bundles without rupture.

bundles, as show in Figure 7C. Here, the maximum stress is 383.9 MPa, the maximum force of the PL and AM bundles are 430N and 156N, as shown in Figure 8A, the maximum moment of the PL bundle is 13.2 Nm, and the maximum moment of the AM bundle is 5.7 Nm, as shown in Figure 8C.

4 Discussion

This study provided an anatomic ACL model that accurately simulated the ACL injury process and investigated its injury mechanism. In the simulation, stress concentration was predicted at the top of the PL bundle and was validated by a badminton sportsman suffering knee joint injury when undergoing an internal rotation and varus combined movement. His injury was diagnosed by MR imaging and arthroscopic examination. The varus and internal rotations simulated in this study present how the force conducts both axial torsional and tensile forces on the ACL. Internal tibial rotation was found to be the major contributor of ACL loading leading to injury in these simulations, with stresses on PL bundles due to internal rotation predicted to be the maximum contributing factor as shown in Figure 7. These results correspond with previous studies on knee joint that indicate internal tibial rotation significantly enhances ACL strain compared with external rotation [15,16,17]. Internal tibial rotation generates an anterior tibial translation that increases ACL loading [18]. This anterior tibial translation is a notable contributing factor to ACL strain [19]. This is the essence of the mechanism of ACL injury

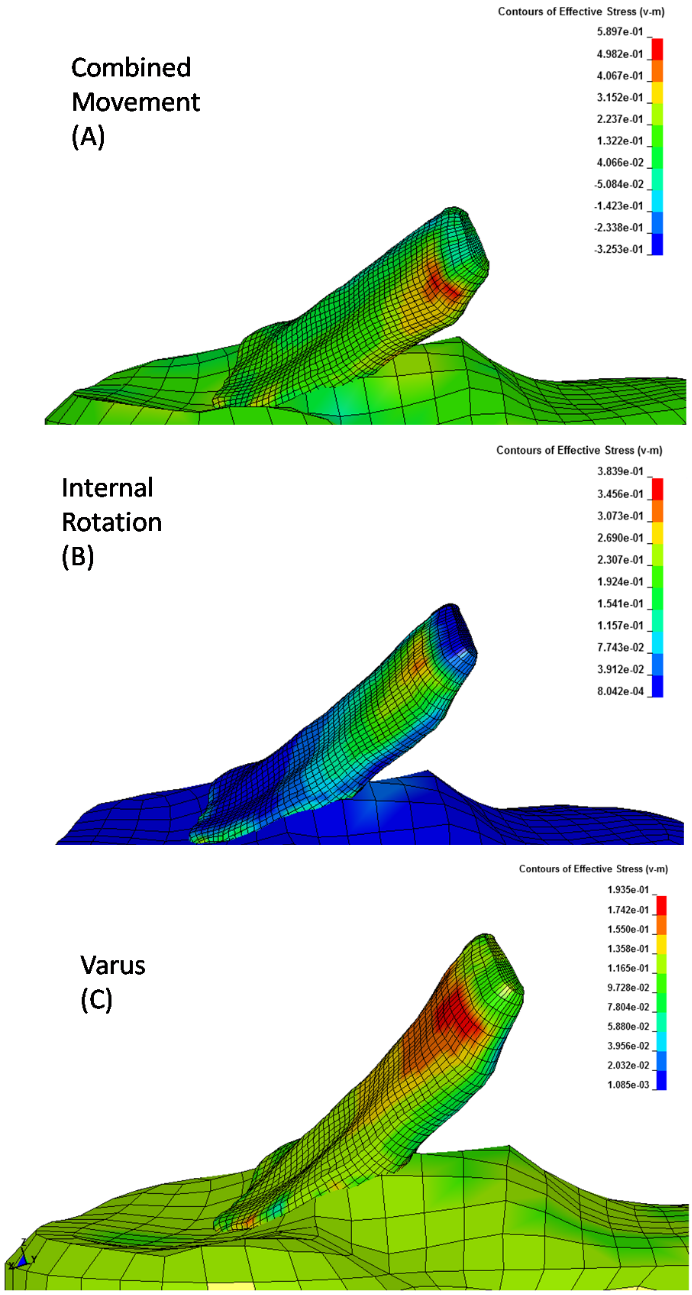

Figure 7: (A) Stress Contour of Von-mises Stress under Combined movements, (B) Stress Contour of Von-mises Stress under Internal Rotational Movement, (C) Stress Contour of Von-mises Stress under Individual Varus Movement.

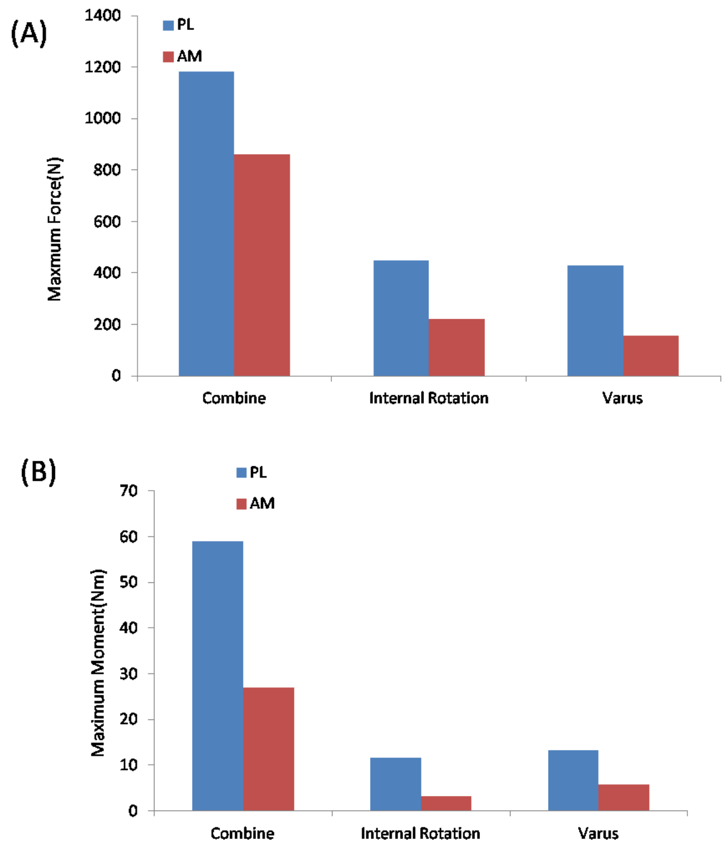

Figure 8: (A) Maximum Force of PL and AM bundles under Combined movements, Internal Rotational Movement and Varus Movement. (B) Maximum Moment of PL and AM bundles under Combined movements, Internal Rotational Movement and Varus Movement.

caused by internal tibial rotation.

ACL has a complex fiber structure that enables proper function in complex knee joint movement that usually combines various movement patterns. The anatomic factors, such as fiber orientation and attachment location, contributed markedly to the functional specificity of these fiber bundles. Even in uniaxial tibial movement, elongations of the fiber bundles in ACL are different [1]. The fiber orientation of AM and PL bundles are significantly different. That means the function and biomechanical property of them have specificity. Akgun [20] reported that AM bundle play major restrictive roles in the knee anterior drawer test, while the PL bundles play the major restrictive role in the pivot shift test.

To present the anisometry of the ACL, the orientation of ACL solid hexahedral elements were built based on anatomical ACL fiber orientation and the FE modeling contact surfaces were the same as the femoral attachment shape of the ACL. However, the anisometry of the ACL could also be incorporate into the model as an anisotropic material [7], in theory, the anisotropic material model would be higher biofidelity in ACL simulation, to verify the different material parameters in transverse and axial of anisotropic ACL, the biomechanical experiments implement should measure both transverse and axial biomechanical response simultaneously, then the material parameter would be caculated in optimization of Finite element modeling, Unfortunately there's no such biomechanical implement, as a compromise, in this model, the anisometry of ACL fiber bundles was presented the Ogden hyper-elastic material model. This material properties was also utilized in Song's study to the force and stress distribution within the anteromedial (AM) and posterolateral (PL) bundles of the anterior ACL in response to an anterior tibial load [5].

In this study, more biofidelity ACL fiber orientation and optimal simulation of complex movements was developed in this FE modeling, which is based on the previous literature and detailed anatomical observations. NSGA-II optimization was utilized to minimize the error between experiments and simulations. FE modeling was performed with the FE code LS-DYNA, an explicit, large deformation, Lagrangian dynamic finite element program that is used widely for dynamic crash simulation and for nonlinear structure analysis. As predicted by the model, stress concentrated at the top of PL bundles in combined movements of knee varus rotation, internal rotation and slight flexion. This prediction had been validated. These predictions imply that individual varus rotation under slight flexion did not provide a major stress to ACL directly, but added tension by alteration of the ACL fiber direction that made it more vulnerable to anterior shear force. Conversely, internal tibial rotation was the major contributor to ACL tension that led to injury. This Analysis provides a reference for orthopedists to aid in the diagnosis of ACL injury. In addition, it will have more crucial benefits to sports medicine to prevent sports-related injury in athletic training and will provide biomechanical evidence for the adjustment of kinematic training patterns.

Acknowledgement: The authors gratefully acknowledge the support of the National Education Department Key Laboratory through the research projects cqu-moekl-br-2011-3 and 2012QNZT161. The authors thank Dr. Hu, J. in University of Michigan for help with algorithm and analysis.

References

1. Hewett, T. E., Myer, G. D. et al. (2005) Biomechanical measures of neuromuscular control and valgus loading of the knee predict anterior cruciate ligament injury risk in female athletes A prospective study. *The American journal of sports medicine*, 33, 4, 492-501.

2. McLean, S. G., Huang, X. et al. (2005) Association between lower extremity posture at contact and peak knee valgus moment during sidestepping: implications for ACL injury. *Clinical Biomechanics*, 20, 8, 863-870.

3. Woo, S. L.-Y., Abramowitch, S. D. et al. (2006) Biomechanics of knee ligaments: injury, healing, and repair. *Journal of Biomechanics*, 39, 1, 1-20.

4. Limbert, G., Taylor, M. et al. (2004) Three-dimensional finite element modelling of the human ACL: simulation of passive knee flexion with a stressed and stress-free ACL. *Journal of Biomechanics*, 37, 11, 1723-1731.

5. Song, Y., Debski, R. E. et al. (2004) A three-dimensional finite element model of the human anterior cruciate ligament: a computational analysis with experimental validation. *Journal of Biomechanics*, 37, 3, 383-390.

6. Peña, E., Calvo, B. et al. (2006) A three-dimensional finite element analysis of the combined behavior of ligaments and menisci in the healthy human knee joint. *Journal of Biomechanics*, 39, 9, 1686-1701.

7. Park, H.-S., Ahn, C. et al. (2010) A knee-specific finite element analysis of the human anterior cruciate ligament impingement against the femoral intercondylar notch. *Journal of Biomechanics*, 43, 10, 2039-2042.

8. Gabriel, M. T. (2003) Distribution of in situ forces in the anterior cruciate ligament in response to rotatory loads. *Journal of Orthopdedic Research*.

9. Hosseini, A., Thomas, J. et al. (2009) In vivo anterior cruciate ligament elongation in response to axial tibial loads. *J Orthop Sci* , 14, 9.

10. Amiri, S. (2011) A multiple-bundle model to characterize the mechanical behavior of the cruciate ligaments. *the knee*.

11. Hu, J., Klinich, K. D. et al. (2009) Quantifying dynamic mechanical properties of human placenta tissue using optimization techniques with specimen-specific finite-element models. *Journal of Biomechanics*, 42, 15, 2528-2534.

12. Guan, F., Han, X. et al. (2010) Application of Optimization Methodology and Specimen-Specific Finite Element Models for Investigating Material Properties of Rat Skull. *Annals of Biomedical Engineering*, 39, 1, 85-95.

13. Noyes, F. R. & Grood, E. S. (1976) The strength of the anterior cruciate ligament in humans and Rhesus monkeys. *The Journal of bone and joint surgery. American volume*, 58, 8, 1074-1082.

14. Deb, K., Pratap, A. et al. (2002) A fast and elitist multiobjective genetic algorithm: NSGA-II. *Evolutionary Computation, IEEE Transactions on*, 6, 2, 182-197.

15. Markolf, K. L., O'Neill, G. et al. (2004) Effects of applied quadriceps and hamstrings muscle loads on forces in the anterior and posterior cruciate ligaments. *Am J Sports Med*, 32, 5, 1144-9.

16. Quatman, C. E., Quatman-Yates, C. C. et al. (2010) A ′plane′ explanation of anterior cruciate ligament injury mechanisms: a systematic review. *Sports Med*, 40, 9, 729-46.

17. Oh, Y. K., Kreinbrink, J. L. et al. (2012) Effect of axial tibial torque direction on ACL relative strain and strain rate in an in vitro simulated pivot landing. *J Orthop Res*, 30, 4, 528-34.

18. LaPrade, R. F., Wentorf, F. A. et al. (2007) A prospective magnetic resonance imaging study of the incidence of posterolateral and multiple ligament injuries in acute knee injuries presenting with a hemarthrosis. *Arthroscopy*, 23, 12, 1341-7.

19. Yu, B. & Garrett, W. E. (2007) Mechanisms of non-contact ACL injuries. *Br J Sports Med*, 41 Suppl 1, i47-51.

20. Akgun, I., Unlu, M. C. et al. (2009) Evaluation of the functional effects of anterior cruciate ligament bundles: a cadaveric experiment. *J Knee Surg*, 22, 4, 317-24.